

Concurrent inhibition of oncogenic and wild-type RAS-GTP for cancer therapy

Mallika Singh

mallika@revmed.com

Revolution Medicines

Matthew Holderfield

Department of Biology, Revolution Medicines

Bianca Lee

Department of Biology, Revolution Medicines

Jingjing Jiang

Department of Biology, Revolution Medicines

Aidan Tomlinson

Department of Chemistry, Revolution Medicines

Kyle Seamon

Department of Biology, Revolution Medicines

Alessia Mira

Department of Molecular Biotechnology and Health Sciences, Molecular Biotechnology Center, University of Torino

Enricho Patrucco

Department of Molecular Biotechnology and Health Sciences, Molecular Biotechnology Center, University of Torino

Grace Goodhart

Department of Surgery, University of Cincinnati

Julien Dilly

Department of Medical Oncology, Dana-Farber Cancer Institute

Yevgeniy Gindin

Department of Biology, Revolution Medicines

Nuntana Dinglasan

Department of Biology, Revolution Medicines

Ying Wang

Department of Biology, Revolution Medicines

Lick Pui Lai

Department of Biology, Revolution Medicines

Shurui Cai

Department of Biology, Revolution Medicines

Lingyan Jiang

Department of Biology, Revolution Medicines

Yu Yang

Department of Biology, Revolution Medicines

Nicole Nasholm

Department of Biology, Revolution Medicines <https://orcid.org/0000-0002-5451-4985>

James Evans

Department of Biology, Revolution Medicines

Nilufar Montazer

Department of Biology, Revolution Medicines

Oliver Lai

Department of Biology, Revolution Medicines

Jade Shi

Department of Biology, Revolution Medicines

Ethan Ahler

Department of Biology, Revolution Medicines

Stephanie Chang

Department of Nonclinical Development and Clinical Pharmacology, Revolution Medicines

Anthony Salvador

Department of Chemistry, Revolution Medicines

Abby Marquez

Department of Chemistry, Revolution Medicines

Jim Cregg

Department of Chemistry, Revolution Medicines

Yang Liu

Department of Chemistry, Revolution Medicines

Anthony Milin

Department of Chemistry, Revolution Medicines <https://orcid.org/0000-0002-1923-7441>

Anqi Chen

Department of Chemistry, Revolution Medicines

Tamar Bar Ziv

Department of Chemistry, Revolution Medicines

Dylan Parsons

Department of Chemistry, Revolution Medicines

John Knox

Department of Chemistry, Revolution Medicines

Jennifer Roth

Broad Institute of MIT and Harvard <https://orcid.org/0000-0002-5117-5586>

Matthew Rees

Broad Institute <https://orcid.org/0000-0002-2987-7581>

Melissa Ronan

Broad Institute of MIT and Harvard <https://orcid.org/0000-0003-4269-1404>

Antonio Cuevas-Navarro

UCSF <https://orcid.org/0000-0001-6208-6944>

Feng Hu

Human Oncology and Pathogenesis Program, Memorial Sloan Kettering Cancer Center

<https://orcid.org/0000-0001-9605-7594>

Piro Lito

Memorial Sloan-Kettering Cancer Center <https://orcid.org/0000-0003-2196-3503>

David Santamaria

Molecular Mechanisms of Cancer Program, Centro de Investigación del Cáncer, CSIC-Universidad de Salamanca

Andrew Aguirre

Dana-Farber Cancer Institute <https://orcid.org/0000-0002-0701-6203>

Andrew Waters

Department of Surgery, University of Cincinnati

Channing Der

<https://orcid.org/0000-0002-7751-2747>

Chiara Ambrogio

University of Torino <https://orcid.org/0000-0003-4122-701X>

Zhengping Wang

Department of Nonclinical Development and Clinical Pharmacology, Revolution Medicines

Adrian Gill

REVOLUTION Medicines, Inc.

Elena Koltun

Department of Chemistry, Revolution Medicines

Jacqueline Smith

Department of Biology, Revolution Medicines

David Wildes

Department of Biology, Revolution Medicines

Biological Sciences - Article**Keywords:**

Posted Date: July 7th, 2023

DOI: <https://doi.org/10.21203/rs.3.rs-3122478/v1>

License: © ⓘ This work is licensed under a Creative Commons Attribution 4.0 International License.

[Read Full License](#)

Additional Declarations: Yes there is potential Competing Interest. .H., B.J.L., J.J, A.T., K.S., Y.G., N.D., Y.W., L.P.L., S.C., L.J., Y.C.Y, N.N., J.W.E., N.M., O.L., J.S., E.A., S.C., R.Z., A.S., A.M., J.C., Y.L., A.M., A.C., T.B.Z., D.P., J.E.K., Z.W., A.L.G., E.S.K., J.A.M.S., D.W. & M.S. are employees of Revolution Medicines; A.J.A. has consulted for Anji Pharmaceuticals, Affini-T Therapeutics, Arrakis Therapeutics, AstraZeneca, Boehringer Ingelheim, Oncorus, Inc., Merck & Co., Inc., Mirati Therapeutics, Nimbus Therapeutics, Plexium, Revolution Medicines, Reactive Biosciences, Riva Therapeutics, Servier Pharmaceuticals, Syros Pharmaceuticals, T-knife Therapeutics, Third Rock Ventures, and Ventus Therapeutics; A.J.A. holds equity in Riva Therapeutics; A.J.A. has research funding from Bristol Myers Squibb, Deerfield, Inc., Eli Lilly, Mirati Therapeutics, Novartis, Novo Ventures, Revolution Medicines, and Syros Pharmaceuticals; C.A. received research fees from Revolution Medicines, Aelin Therapeutics, Verastem, Roche and Boehringer-Ingelheim

Version of Record: A version of this preprint was published at Nature on April 8th, 2024. See the published version at <https://doi.org/10.1038/s41586-024-07205-6>.

Abstract

RAS oncogenes (collectively *NRAS*, *HRAS*, and especially *KRAS*) are among the most frequently mutated genes in cancer, with common driver mutations occurring at codons 12, 13 and 61¹. Small molecule inhibitors of the *KRAS*^{G12C} oncoprotein have demonstrated clinical efficacy in patients with multiple cancer types and have led to regulatory approvals for the treatment of non-small-cell lung cancer (NSCLC)^{2,3}. Nevertheless, *KRAS*^{G12C} mutations account for only ~14% of *KRAS* mutated cancers⁴ and there are no approved *KRAS* inhibitors for the majority of patients with tumors harboring other common *RAS* mutations. Here, we describe RMC-7977, a reversible, tri-complex *RAS* inhibitor with broad spectrum activity for both mutant and wild-type (WT) *KRAS*, *NRAS*, and *HRAS* variants (a *RAS*^{MULTI}(ON) inhibitor). Preclinically, RMC-7977 demonstrated potent activity against *RAS*-addicted tumors carrying various *RAS* genotypes, particularly cancer models with *KRAS* codon 12 mutations (*KRAS*^{G12X}). RMC-7977 led to tumor regressions and was well tolerated in diverse *RAS*-addicted preclinical cancer models. Additionally, RMC-7977 inhibited the growth of *KRAS*^{G12C} cancer models that are resistant to *KRAS*^{G12C} inhibitors due to restoration of *RAS* pathway signaling. Thus, *RAS*^{MULTI}(ON) inhibitors can target multiple oncogenic and WT *RAS* isoforms and hold the potential to treat a wide range of *RAS*-addicted cancers with high unmet clinical need. A related *RAS*^{MULTI}(ON) inhibitor, RMC-6236, is currently under clinical evaluation in patients with *KRAS*^{G12X} mutant solid tumors (NCT05379985).

Main

RAS genes encode small GTPase proteins that regulate cell proliferation in response to growth factor stimuli^{1,5}. Cancer-associated *KRAS* mutations are found frequently in NSCLC, colorectal cancers (CRC), and pancreatic ductal adenocarcinoma (PDAC)², the top three leading causes of cancer deaths in the United States⁶. These activating mutations drive tumor progression by stabilizing the active, GTP-bound state of *RAS* proteins and thereby increasing oncogenic flux through downstream effectors⁷. Analysis of CRISPR-Cas9 functional genetic screening data demonstrated that *KRAS*-mutated cancer cell lines are highly sensitive to disruption of the *KRAS* locus (Extended Data Fig. 1a), and *KRAS* mutation status was the only genetic feature exhibiting a significant correlation with *KRAS* dependency (Extended Data Fig. 1b). Similar results were observed for the other *RAS* isoforms, *NRAS* and *HRAS* in *NRAS*- and *HRAS*-mutated lines, respectively (Extended Data Fig. 1c-f). Furthermore, *KRAS* mutations at position 12 are both the most frequent *KRAS* alterations and associated with the highest degree of *KRAS* dependency as compared to other *KRAS* mutations (Fig. 1a). This result suggests that while many mutations at *KRAS* codons 12, 13, or 61 have transforming potential^{8,9}, not all *KRAS* mutations are associated with equivalent *KRAS* oncogene dependence. Additionally, these data suggest that *KRAS*^{G12X} mutation is a genetic marker of *RAS* oncogene addiction (Extended Data Fig. 1g) and highlight a patient population that may derive particularly high benefit from a targeted inhibitor of these oncogenic *RAS* variants.

RMC-7977 discovery and development

RAS proteins have historically been recalcitrant drug targets^{2,3}, though progress in targeting the inactive, GDP-bound state of KRAS^{G12C} has resulted in two regulatory approvals (sotorasib and adagrasib)^{10,11}. We recently described RMC-4998 and RMC-6291, two covalent tri-complex inhibitors designed to target the active-state of KRAS^{G12C}¹². These macrocyclic compounds were derived from sangliferin A, a natural product that binds to cyclophilin A (CYPA) with high affinity¹³. Upon binding CYPA, these compounds generate a neomorphic interface with affinity for active KRAS and achieve high selectivity for KRAS^{G12C} via covalent modification of the reactive thiol group introduced by the oncogenic mutation. The resulting CYPA:compound:KRAS tri-complex sterically blocks KRAS-effector interactions and disrupts downstream signaling.

Most RAS oncoproteins with missense mutations are not amenable to selective covalent targeting but could be susceptible to non-covalent inhibition by tri-complex formation with CYPA. We postulated that we could use structure-guided design to optimize the neomorphic interface between CYPA and RAS and generate a reversible inhibitor with broad activity against the active states of multiple RAS variants. Tri-complex formation requires two distinct binding events (Fig. 1b). First, compound binds to CYPA to form the binary complex (K_D1). The binary CYPA:compound complex then binds to active RAS (K_D2) to form a tri-complex structure in which CYPA sterically occludes RAS:effector interactions (Extended Data Fig. 2a-d). Both binding events are essential for tri-complex formation, and we sought to optimize both K_D1 and K_D2 to increase the potency of RAS inhibition, focusing initially on KRAS^{G12V} as a representative oncogenic mutant.

We selected Compound 1 (Fig. 1c) from the previous study¹² as a promising starting point for design of reversible and orally bioavailable inhibitors of the active state of RAS. Compound 1 contains a CYPA-binding motif (Extended Data Table 1, $K_D1 = 862$ nM) and forms reversible tri-complexes with KRAS^{G12V} ($K_D2 = 6,550$ nM) that weakly disrupt the binding to the RAS-binding domain (RBD) of BRAF ($EC_{50} = 4,400$ nM). Compound 1 is cell-active, inhibiting RAS pathway activation (pERK $EC_{50} = 632$ nM and proliferation $EC_{50} = 965$ nM) in Capan-1 cells (PDAC, KRAS^{G12V}; Extended Data Table 1). Introduction of a thiazole moiety and concomitant scaffold rigidification through rotatable bond reduction and control of hydrogen bond donor count in the side chain yielded Compound 2, with improved affinity for CYPA ($K_D1 = 330$ nM) and improved cellular potency (pERK $EC_{50} = 31.6$ nM; proliferation $EC_{50} = 149$ nM; Extended Data Table 1). Further reduction of peptidic character resulted in Compound 3, with increased binary complex affinity for KRAS^{G12V} ($K_D2 = 818$ nM) as well as improved oral bioavailability in mice (m%F = 43.6), but reduced affinity for CYPA ($K_D1 = 6,270$ nM) and reduced cellular potency (pERK $EC_{50} = 124$ nM; proliferation $EC_{50} = 618$ nM).

To address the reduced CYPA affinity of Compound 3, we introduced a piperazine moiety on the left-hand side of the scaffold to create a cation- π interaction with W121 of CYPA. This modification not only enhanced CYPA binding affinity (Compound 4; $K_D1 = 605$ nM), but also affinity for KRAS^{G12V} ($K_D2 = 292$ nM) and cellular potency (pERK $EC_{50} = 1.94$ nM, proliferation $EC_{50} = 14.2$ nM) (Extended Data Table 1).

Structure-guided optimization of a water network-mediated interaction with the Y32 backbone carbonyl of KRAS bound to a GTP analog (GMPPNP) (Fig. 1d) resulted in RMC-7977, a potent ($K_D1 = 195$ nM; $K_D2 = 85$ nM; pERK $EC_{50} = 2.20$ nM; proliferation $EC_{50} = 0.421$ nM) and orally bioavailable (m%F = 62.7) RAS^{MULTI}(ON) inhibitor (Extended Data Fig. 2g,h and Extended Data Table 1). RMC-7977 makes a cation-pi interaction between CYPA and the piperazine moiety, and additional hydrophobic and polar interactions are observed, including with the catalytic R55 (Fig. 1e).

Although neither RMC-7977 nor CYPA alone exhibited any measurable binding to GMPPNP-KRAS (Extended Data Fig. 2i,j), RMC-7977 makes multiple pi-pi and hydrophobic contacts with RAS in the SWI and SWII region once the tri-complex is formed (Fig. 1f). All residues in the binding site are identical among HRAS, KRAS, NRAS (Extended Data Fig. 2e), and RMC-7977 is equipotent across these RAS isoforms (Extended Data Table 1). K_D2 measurements for all three WT RAS proteins were approximately 100 nM (K_D2 for KRAS = 120 nM, NRAS: 98 nM, and HRAS = 90 nM).

A high-resolution co-crystal structure of RMC-7977 bound to CYPA and GMPPNP-bound KRAS was solved and shows a non-covalent tri-complex with an unoccupied groove containing the common oncogenic residues, G12, G13, and Q61, providing a structural basis for the ability of RMC-7977 to bind these variants (Fig. 1g). Further, RMC-7977 exhibited a consistent binding mode across all KRAS^{G12X} mutants tested (Extended Data Fig. 2f). K_D2 values for the most common oncogenic RAS variants were all within 3-fold of those for WT proteins (Fig. 1h and Extended Data Table 1). The ability of tri-complex formation to sterically disrupt effector binding for the various mutants was also measured, revealing a good correlation between the K_D2 measurements and the biochemical EC_{50} values for RAS-RAF disruption.

We used a live-cell nano-BRET kinetic assay to show that RMC-7977 induced equally rapid ($t_{1/2} < 5$ min., Fig. 2a) association between KRAS and CYPA and dissociation of the CRAF RBD from KRAS, consistent with direct targeting of the active-state of RAS in cells accompanied by steric inhibition of protein-protein effector engagement. EC_{50} measurements in this assay were in the single-digit nanomolar range across a panel of WT, G12, G13, and Q61-mutant KRAS proteins (Fig. 2b). Notably, the cellular potency for WT KRAS was modestly lower than potency for the oncogenic variants. Further, the cellular potencies for KRAS:CYPA association were approximately 5-50x higher than the corresponding biochemical K_D2 measurements (Extended Data Table 1). An increase in cellular potency compared to biochemical potency is expected based on the tri-complex mechanism of action, in which binding to abundant CYPA drives high intracellular concentrations of CYPA:RMC-7977 binary complexes, as is evidenced by accumulation of RMC-7977 in a CYPA-dependent manner in AsPC-1 cells (Extended Data Fig. 3a). Furthermore, biochemical and cellular potencies correlate well when adjusted to reflect the estimated intracellular concentration of binary complexes formed in cells (Extended Data Fig. 3b,c).

To verify that formation of the CYPA:RMC-7977 binary complex is essential for cellular activity, we used a competitive CYPA inhibitor¹⁴ or genetically knocked out *PPIA*, the gene that encodes CYPA. These studies confirm that CYPA binding is required for inhibition of RAF-MEK-ERK signaling and proliferation by RMC-

7977 in NCI-H441 (KRAS^{G12V}, NSCLC) and AsPC-1 (KRAS^{G12D}, PDAC) cells (Extended Data Fig. 3d-g). As a control, disruption of the *PPIA* locus did not affect sensitivity to the MEK1/2-selective inhibitor, trametinib, which does not rely on the tri-complex mechanism of action (Extended Data Fig. 3h,i). We further investigated whether exogenous CYPA expression could restore RMC-7977 sensitivity in NCI-H358 (KRAS^{G12C}, NSCLC) cells lacking *PPIA*. We investigated two clones expressing either low or high CYPA levels through a doxycycline-inducible promoter (Extended Data Fig. 4a). Inhibition of pERK and proliferation was CYPA dependent, and CYPA high cells were 3- and 8-fold more sensitive to RMC-7977 inhibition of signaling and cell proliferation, respectively, compared to CYPA low cells (Fig. 2c, Extended Data Fig. 4b). RMC-7977 accumulation was significantly greater in CYPA high compared to CYPA low cells treated with 10 nM RMC-7977, with no difference at 1 μ M at which concentration binding to cellular CYPA is estimated to approach saturation (Fig. 2d). Collectively these observations suggest that the cellular potency of RMC-7977 is dependent on intracellular concentration of binary complexes, driven by intracellular CYPA protein expression. CYPA is highly abundant in cells (median concentration = 12.3 μ M) as measured across a panel of 15 cell lines (Extended data Fig. 4c), and CYPA expression was higher in cell line-derived xenograft (CDX) tumors *in vivo* compared to the corresponding cells cultured *in vitro* (Extended Data Fig. 4d). Finally, CYPA is abundantly expressed across cancer types and exhibits low inter-patient variation in expression¹², suggesting that tumor expression of CYPA is unlikely to be limiting for RMC-7977 potency.

Although RMC-7977 exhibited similar activity for WT and mutant RAS variants in biochemical assays and the live-cell nano-BRET assay, many factors can influence the downstream consequences of RAS inhibition in cells. To assess the spectrum of RMC-7977 activity against common KRAS variants in cells, we evaluated a panel of matched mouse embryo fibroblasts (MEFs) null for all three *Ras* genes (RAS-less) where proliferation was restored with ectopic expression of WT or mutationally-activated *KRAS* or *BRAF*^{V600E} (Fig. 2e)¹⁵. RMC-7977 suppressed pERK in all *KRAS*-expressing cells, but not *BRAF*^{V600E}-expressing RAS-less MEFs, which lack all RAS proteins and are not RAS dependent, indicating that pERK suppression is *KRAS*-dependent. Interestingly, we noted that pERK suppression by RMC-7977 typically appeared complete across cells expressing various *KRAS*^{G12X} mutants, but consistently reached a plateau in WT *KRAS*, *KRAS*^{G12A}, *KRAS*^{Q61L}, *KRAS*^{Q61R}, *KRAS*^{G13D}, and *KRAS*^{A146T} cells; in contrast and as expected, trametinib reduced pERK similarly in all cells, including the *BRAF*^{V600E} MEFs (Extended Data Fig. 5c). These differences indicate that *KRAS* genotype could affect cellular response to direct RAS inhibition, and that the cellular response to RMC-7977 inhibition is not equivalent to that of MEK inhibition.

We also compared RMC-7977 activity in cancer cells harboring various activating mutations in the RAS pathway, specifically oncogenic variants of *KRAS*, *NRAS*, *EGFR*, or *BRAF*. RAS-dependent (*KRAS*, *NRAS*, or *EGFR* mutated) cancer cells treated with RMC-7977 exhibited concentration-dependent inhibition of downstream signaling markers, including phosphorylation of RAF, ERK, and the ERK substrate RSK, and inhibition of proliferation in the low nanomolar range (Fig. 2f,g). *KRAS* mutant cells also showed durable pathway suppression up to 48 h, as well as apoptosis induction indicated by increased PARP cleavage

(Extended Data Fig. 5a,b). No inhibition by RMC-7977 was observed in RAS-independent *BRAF*^{V600E}-mutant A375 cells (Fig. 2f,g).

RMC-7977 is broadly active in RAS-addicted cancers

We next employed a cell viability assay in 818 human tumor cell lines of different genetic and histological subtypes in a pooled, multiplexed format (PRISM assay) to identify genetic features associated with RMC-7977 sensitivity or resistance. Oncogenic *KRAS* mutation status provided the most significant genetic marker of sensitivity to RMC-7977 (Fig. 3a). Similar results were observed for *NRAS* mutations, though no correlation with *HRAS* mutation status was detected due to the low representation of *HRAS* mutations (Extended Data Fig 6a,b). Unsurprisingly, among cell lines with *BRAF* mutations, *BRAF* Class I V600 mutations were the most abundantly represented and clearly associated with resistance. Cell lines with less common Class II or III mutations, which remain somewhat dependent on upstream RAS signaling and frequently co-occur with RAS mutations, were often sensitive to RMC-7977, as were many unclassified *BRAF* mutations (Extended Data Fig. 6c). As predicted by *KRAS* gene dependency (Fig. 1a), *KRAS* mutated cell lines were more sensitive to RMC-7977 compared to cell lines with other RAS pathway aberrations and cells with no identifiable RAS pathway alteration. Moreover, *KRAS*^{G12X} (and *NRAS* mutant) cells were particularly sensitive to RMC-7977 as compared to other RAS pathway genotypes (Extended Data Fig. 6d).

We then selected a second, focused panel of 183 individually arrayed human cancer cell lines enriched for RAS and RAS pathway mutations to interrogate RMC-7977 potency. *KRAS*^{G12X} mutant cells were again the most sensitive, followed by *NRAS*-, *HRAS*-, and non-G12 *KRAS*-mutant cell lines (Extended Data Fig. 6e). *KRAS*^{G12X} mutant cell lines were highly sensitive with a median EC₅₀ of 2.40 nM. By comparison, non-G12 mutant *KRAS* cell lines showed ~10-fold reduced sensitivity (median EC₅₀ = 25.1 nM) (Fig. 3b). Taken together, these data are concordant with our genetic analysis of *KRAS* dependence and support the on-target pharmacological activity of RMC-7977. In addition, *NRAS* and *HRAS* mutant cell lines (median EC₅₀ = 6.76 nM), and cell lines with mutationally activated RTKs also responded to RMC-7977 inhibition, including those with mutations or fusions of *EGFR*, *ERBB3*, *FGFR1*, *FGFR2*, *FGFR3*, *ROS1*, *RET*, *NTRK1*, and *ALK* (median EC₅₀ = 6.14 nM), and cell lines with WT *MET* gene amplification (median EC₅₀ = 6.61 nM, Extended Data Fig. 6f). Cell lines with *NF1* loss-of-function and *PTPN11* mutations, which each cause activation of WT RAS signaling, were moderately sensitive (median EC₅₀ = 28.1 nM).

We then assessed the pharmacodynamic and anti-tumor activity of RMC-7977 *in vivo* in the NCI-H441 CDX model of non-small cell lung cancer (*KRAS*^{G12V}, NSCLC). The relationship between the total tumor concentration of RMC-7977 and inhibition of a RAS pathway transcriptional target, *DUSP6*, in tumor lysates yielded an EC₅₀ of 130 nM (Extended Data Fig. 7a), consistent with the measured *KRAS*^{G12V} K_D2 of 85 nM (Extended Data Table 1), and with the model for tri-complex RAS inhibition discussed above. A single oral dose of 10 mg/kg RMC-7977 was sufficient to maximally suppress tumor *DUSP6* levels (91%) at 8 h, which partially recovered over 48 h, concordant with the decrease in RMC-7977 tumor

concentrations (Fig. 3c). Prolonged RMC-7977 exposure in tumors was observed in this and other subcutaneously implanted xenograft tumor models, resulting in a ~2- to 3-fold increase in overall exposure (AUC_{0-last}) in subcutaneous tumors compared to blood (Extended Data Fig. 7b). Repeated daily administration of RMC-7977 at 10 mg/kg was well-tolerated based on body weights (Extended Data Fig. 7c) and resulted in 83% mean tumor regression following 28 days treatment in the NCI-H441 model. Notably, we saw similar anti-tumor activity following RMC-7977 treatment across a larger panel of 15 PDAC, CRC, and NSCLC CDX and patient-derived (PDX) models bearing $KRAS^{G12X}$ mutations and co-mutations representative of the genomic landscape of patients with $KRAS$ mutant cancers (Fig. 3e). RMC-7977 treatment resulted in mean tumor regression in 9/15 (60%) models after a 4 to 6-week treatment period (Fig. 3e) and was well tolerated in all (Extended Data Fig. 7c). Importantly, when we continued RMC-7977 treatment in these xenograft models for up to 90 days, the anti-tumor activity of RMC-7977 was found to remain significantly durable as the majority of regressions and even cytostatic responses were maintained. While the controls exhibited a short median time to tumor doubling of 7 days, RMC-7977 treated tumors did not reach a median time to tumor doubling (defined as tumor progression) on treatment in a Kaplan-Meier analysis of these results (Fig. 3f; Cox Proportional Hazard Ratio 0.004, 95% interval 0.0011-0.0191, $P < 1 \times 10^{-12}$).

MEK and ERK inhibitors have undergone extensive clinical testing as monotherapies or in combinations with other RAS pathway inhibitors in patients with $KRAS$ or $NRAS$ mutated cancers¹⁶. Despite encouraging preclinical results, these therapeutic strategies have been unsuccessful in the clinic¹⁷⁻¹⁹ to date, with therapeutic efficacy likely compromised by dose-limiting toxicities²⁰⁻²². We compared the anti-tumor activity of RMC-7977 to cobimetinib (MEK inhibitor), RMC-4550 (SHP2 inhibitor), and the combination thereof in three $KRAS^{G12X}$ models. At well tolerated doses, RMC-7977 induced deep regressions in all three models, whereas MEK and SHP2 inhibitors alone or in combination achieved only modest tumor growth inhibition at well tolerated and translatable doses (Fig. 3g). In these preclinical models of $KRAS^{G12X}$ mutant cancers, direct targeting of active RAS with RMC-7977 elicited a differentiated and superior anti-tumor activity profile as compared to upstream and/or downstream vertical inhibition of the primary oncogenic RAS driver.

There are several potential mechanistic explanations for why RMC-7977 elicits significantly greater anti-tumor activity in $KRAS^{G12X}$ -driven cancers compared to agents targeting upstream and/or downstream nodes in the RAS pathway. Directly targeting the RAS oncoprotein itself may exploit the high degree of oncogene addiction of $KRAS^{G12X}$ (and $NRAS$) mutated cancer cells to a greater degree than targeting upstream and downstream signaling proteins (e.g. SHP2, MEK1/2, and ERK1/2). Furthermore, while MEK inhibition did not distinguish between WT and mutant RAS variants (Extended Data Fig. 5c), RMC-7977 exhibited modestly lower potency and incomplete WT RAS suppression compared to $KRAS^{G12X}$ in cells (Fig. 2b,e and Extended Data Table 1). Additionally, the slow elimination of RMC-7977 observed in subcutaneous xenograft tumors relative to blood suggests differential effective distribution to tumors, which may contribute to a wider therapeutic index. Of note, *CYPA* mRNA expression is reportedly induced by hypoxia under control of *HIF-1a* and plays a critical role in tumorigenesis^{23,24}. Consistent with these

reports, subcutaneous xenograft tumors express elevated CYPA protein compared to cells grown *in vitro* under normoxic conditions (Extended Data Fig. 4d) and CYPA mRNA expression is increased in tumor cells²⁵. Collectively these data support the notion that CYPA is critical for tumor maintenance and could affect tumor distribution and cellular retention of tricomplex inhibitors.

RMC-7977 can overcome clinically relevant resistance mechanisms to KRAS^{G12C}(OFF) inhibitors

While inactive-state KRAS^{G12C} inhibitors provide short-term therapeutic benefit for some, patients, most eventually relapse through acquired genetic or adaptive mechanisms of resistance²⁶⁻²⁹. Ryan et al. have reported that adaptive feedback reactivation of upstream RTK signaling through WT RAS limits the activity of KRAS^{G12C} inhibitors²⁹. We observed analogous results in KRAS^{G12D} mutant PDAC cell lines treated with the KRAS^{G12D} selective inhibitor, MRTX1133, where pERK suppression seen at 2 h rebounded by 48 h after treatment. We hypothesized that RMC-7977 could address adaptive RAS signaling mechanisms that rely on increased active-state WT and mutant RAS proteins. Consistent with this hypothesis, RMC-7977 showed sustained pERK suppression in KRAS^{G12D} mutated PDAC cells in culture for 48 h, suggesting that RAS^{MULTI} inhibition can overcome adaptive feedback observed with mutant-selective inhibitor treatment (Fig. 4a). Similar sustained pERK suppression and induced PARP cleavage were also observed in a KRAS^{G12V} and KRAS^{G12C} mutant cancer cell lines (Extended Data Fig. 5b). To further address whether RMC-7977 can overcome resistance mediated by WT KRAS signaling, we utilized an engineered KRAS^{G12C/WT} loss-of-heterozygosity (LOH) model system in which the endogenous WT *Kras* copy is selectively deleted under control of tamoxifen and the ectopic KRAS^{G12C} allele is constitutively expressed. KRAS^{G12C} cells (LOH) were sensitive to adagrasib and KRAS^{G12C/WT} cells (non-LOH) were resistant, whereas both cell lines were sensitive to RMC-7977 regardless of WT *Kras* expression (Extended Data Fig. 8a,b). We therefore hypothesized that the concurrent suppression of WT and mutant RAS signaling could drive durable anti-tumor responses to RMC-7977 treatment *in vivo*. As described above, a 90-day treatment study in a series of KRAS^{G12X} xenograft models demonstrated marked and significant increase in time to tumor doubling from baseline as compared to controls (Fig. 3f).

The activity of RMC-7977 against multiple forms of oncogenic RAS suggests the potential for therapeutic benefit against resistance mechanisms involving secondary RAS mutations. We recently demonstrated that tri-complex KRAS^{G12C} inhibitors, such as RMC-4998, bind to RAS through a unique mechanism and a binding site distinct from the switch II pocket occupied by inactive-state KRAS^{G12C} inhibitors, such as adagrasib and sotorasib³⁰⁻³². This enables these inhibitors to overcome resistance mediated by switch II pocket binding mutations such as those occurring at positions Y96 and H95²⁶. Consequently, other tri-complex inhibitors, including RMC-7977, would be expected to overcome these same drug binding site mutations. We then tested whether the broad-spectrum RAS inhibitory activity of RMC-7977 could counter additional genetic resistance mechanisms observed in relapsed patients treated with KRAS^{G12C} inhibitors, including secondary oncogenic RAS mutations and RTK activation. Indeed, RMC-7977 inhibited RAS

signaling and growth of an NCI-H358 ($KRAS^{G12C}$ mutated NSCLC) clone with a concurrent $NRAS^{Q61K}$ mutation that emerged in cells grown under continuous exposure to adagrasib *in vitro* (Fig. 4b,c and Extended Data Fig. 8c). RTK amplification and activating mutations can also cause RAS pathway reactivation through WT RAS proteins. We used an engineered system harboring doxycycline-inducible constructs of full-length and fusion RTKs previously detected in patients who progressed on adagrasib or sotorasib treatment²⁶. Overexpression of WT or mutant RTKs in NCI-H358 cells ($KRAS^{G12C}$, NSCLC) conferred significantly reduced sensitivity to adagrasib (proliferation inhibition EC_{50} shift for WT $EGFR$ = 42-fold, $EGFR^{A289V}$ = 153-fold, $HER2$ = 51-fold, $FGFR2$ = 18-fold, RET^{M918T} = 34-fold) while retaining sensitivity to RMC-7977 (Fig. 4d,e and Extended Data Fig. 8d,e). Similar results were observed when oncogenic RTK fusion proteins (EML4-ALK, FGFR3-TACC3, and CCDC6-RET) were exogenously expressed in MIA PaCa-2 cells ($KRAS^{G12C}$, PDAC) (Fig. 4f,g and Extended Data Fig. 8f,g).

Finally, we examined RMC-7977 treatment in a $KRAS^{G12C}$ mutated PDX model derived from a NSCLC patient who had achieved stable disease on sotorasib but quickly relapsed. Genomic alterations in this tumor include amplification of the WT $KRAS$ allele accompanied by increased levels of GTP- $KRAS^{33}$, which contributes to diminished response to sotorasib treatment at 50 mg/kg qd. RMC-7977 administered daily at 10 mg/kg resulted in significant anti-tumor activity, with 90% inhibition of tumor growth observed at D17 of treatment while sotorasib treatment induced only 47% tumor growth inhibition (Fig. 4i). In sum, these data indicate that both adaptive and acquired mechanisms of resistance to $KRAS^{G12C}$ inhibitors that lead to RAS pathway reactivation are susceptible to inhibition by RMC-7977.

RMC-7977 extends the tri-complex inhibitor strategy to non-covalently target the active state of WT and multiple oncogenic RAS variant proteins, with particular activity against the range of common codon 12 mutants, thus offering therapeutic potential for a $RAS^{MULTI}(ON)$ inhibitor across a spectrum of RAS-addicted cancers, including NSCLC, CRC, and PDAC. Evidence of robust, durable anti-tumor activity at well-tolerated doses across various RAS mutant xenograft models provides preclinical validation for the direct targeting of active RAS variants as a desirable therapeutic strategy. Furthermore, we demonstrate that concurrent inhibition of multiple oncogenic RAS variants and WT RAS in the same tumor cell with a reversible RAS^{MULTI} inhibitor such as RMC-7977 can overcome some of the resistance mechanisms recognized to limit the efficacy and durability for inactive-state $KRAS^{G12C}$ inhibitors. The proximity of the RMC-7977 binding site to RAS mutational hotspots (residues G12, G13, and Q61) presents a unique opportunity to expand this approach further by designing additional mutant-selective tri-complex inhibitors. Moreover, RAS^{MULTI} inhibitors could also provide therapeutic benefit in combination with mutant selective $KRAS$ inhibitors to improve anti-tumor response by blocking adaptive pathway reactivation and preventing escape through emergence of secondary oncogenic RAS or RTK mutations. RMC-6236, a first-in-class, clinical-stage RAS^{MULTI} inhibitor, is currently being evaluated (NCT05379985) in patients with solid tumors harboring $KRAS^{G12X}$ mutations.

Declarations

Disclosures and Acknowledgements

D.S. is funded by AECC Excellence Program 2022 (EPAEC222641CICS); A.J.A. has consulted for Anji Pharmaceuticals, Affini-T Therapeutics, Arrakis Therapeutics, AstraZeneca, Boehringer Ingelheim, Oncorus, Inc., Merck & Co., Inc., Mirati Therapeutics, Nimbus Therapeutics, Plexium, Revolution Medicines, Reactive Biosciences, Riva Therapeutics, Servier Pharmaceuticals, Syros Pharmaceuticals, T-knife Therapeutics, Third Rock Ventures, and Ventus Therapeutics; A.J.A. holds equity in Riva Therapeutics; A.J.A. has research funding from Bristol Myers Squibb, Deerfield, Inc., Eli Lilly, Mirati Therapeutics, Novartis, Novo Ventures, Revolution Medicines, and Syros Pharmaceuticals; A.M.W. was supported by a grant from the NCI (K22CA276632-01); C.A. received research fees from Revolution Medicines, Aelin Therapeutics, Verastem, Roche and Boehringer-Ingelheim, and is funded by grants from the Giovanni Armenise–Harvard Foundation, the European Research Council (ERC) under the European Union’s Horizon 2020 research and innovation programme (grant agreement No. [101001288]) and AIRC under IG 2021 - ID. 25737 project. Thank you to Ruiping Zhao and Karl Muonio for technical support for the LCMS experiments and Warp Drive Bio for generating cellular CYP A protein quantification data shown in Extended Data fig 4c.

References

1. Simanshu, D. K., Nissley, D. V. & McCormick, F. RAS Proteins and Their Regulators in Human Disease. *Cell***170**, 17-33 (2017). <https://doi.org:10.1016/j.cell.2017.06.009>
2. Cox, A. D., Fesik, S. W., Kimmelman, A. C., Luo, J. & Der, C. J. Drugging the undruggable RAS: Mission possible? *Nat Rev Drug Discov***13**, 828-851 (2014). <https://doi.org:10.1038/nrd4389>
3. Moore, A. R., Rosenberg, S. C., McCormick, F. & Malek, S. RAS-targeted therapies: is the undruggable drugged? *Nat Rev Drug Discov***19**, 533-552 (2020). <https://doi.org:10.1038/s41573-020-0068-6>
4. Foundation Medicine. FoundationInsights™. Updated: 29 Mar 2022. Accessed: 6 June 2023. Available from: [foundationmedicine.com/service/genomic-data-solutions](https://www.foundationmedicine.com/service/genomic-data-solutions).
5. Malumbres, M. & Barbacid, M. RAS oncogenes: the first 30 years. *Nat Rev Cancer***3**, 459-465 (2003). <https://doi.org:10.1038/nrc1097>
6. Siegel, R. L., Wagle, N. S., Cercek, A., Smith, R. A. & Jemal, A. Colorectal cancer statistics, 2023. *CA Cancer J Clin***73**, 233-254 (2023). <https://doi.org:10.3322/caac.21772>
7. Pylayeva-Gupta, Y., Grabocka, E. & Bar-Sagi, D. RAS oncogenes: weaving a tumorigenic web. *Nat Rev Cancer***11**, 761-774 (2011). <https://doi.org:10.1038/nrc3106>
8. Johnson, C., Burkhart, D. L. & Haigis, K. M. Classification of KRAS-Activating Mutations and the Implications for Therapeutic Intervention. *Cancer Discov***12**, 913-923 (2022). <https://doi.org:10.1158/2159-8290.CD-22-0035>
9. Papke, B. & Der, C. J. Drugging RAS: Know the enemy. *Science***355**, 1158-1163 (2017). <https://doi.org:10.1126/science.aam7622>

10. Janne, P. A. *et al.* Adagrasib in Non-Small-Cell Lung Cancer Harboring a KRAS(G12C) Mutation. *N Engl J Med***387**, 120-131 (2022). <https://doi.org:10.1056/NEJMoa2204619>
11. Skoulidis, F. *et al.* Sotorasib for Lung Cancers with KRAS p.G12C Mutation. *N Engl J Med***384**, 2371-2381 (2021). <https://doi.org:10.1056/NEJMoa2103695>
12. Schulze, C. J. *et al.* Chemical remodeling of a cellular chaperone to target the active state of mutant KRAS. *Science, In Press*.
13. Sanglier, J. J. *et al.* Sanglifehrins A, B, C and D, novel cyclophilin-binding compounds isolated from *Streptomyces* sp. A92-308110. I. Taxonomy, fermentation, isolation and biological activity. *J Antibiot (Tokyo)***52**, 466-473 (1999). <https://doi.org:10.7164/antibiotics.52.466>
14. Mackman, R. L. *et al.* Discovery of a Potent and Orally Bioavailable Cyclophilin Inhibitor Derived from the Sanglifehrins Macrocycle. *J Med Chem***61**, 9473-9499 (2018). <https://doi.org:10.1021/acs.jmedchem.8b00802>
15. Drosten, M. *et al.* Genetic analysis of Ras signalling pathways in cell proliferation, migration and survival. *EMBO J***29**, 1091-1104 (2010). <https://doi.org:10.1038/emboj.2010.7>
16. Hymowitz, S. G. & Malek, S. Targeting the MAPK Pathway in RAS Mutant Cancers. *Cold Spring Harb Perspect Med***8** (2018). <https://doi.org:10.1101/cshperspect.a031492>
17. Collisson, E. A. *et al.* A central role for RAF→MEK→ERK signaling in the genesis of pancreatic ductal adenocarcinoma. *Cancer Discov***2**, 685-693 (2012). <https://doi.org:10.1158/2159-8290.CD-11-0347>
18. Morris, E. J. *et al.* Discovery of a novel ERK inhibitor with activity in models of acquired resistance to BRAF and MEK inhibitors. *Cancer Discov***3**, 742-750 (2013). <https://doi.org:10.1158/2159-8290.CD-13-0070>
19. Peng, S. B. *et al.* Inhibition of RAF Isoforms and Active Dimers by LY3009120 Leads to Anti-tumor Activities in RAS or BRAF Mutant Cancers. *Cancer Cell***28**, 384-398 (2015). <https://doi.org:10.1016/j.ccell.2015.08.002>
20. Daud, A. & Tsai, K. Management of Treatment-Related Adverse Events with Agents Targeting the MAPK Pathway in Patients with Metastatic Melanoma. *Oncologist***22**, 823-833 (2017). <https://doi.org:10.1634/theoncologist.2016-0456>
21. Flaherty, K. T. *et al.* Improved survival with MEK inhibition in BRAF-mutated melanoma. *N Engl J Med***367**, 107-114 (2012). <https://doi.org:10.1056/NEJMoa1203421>
22. Wu, J. *et al.* Characterization and management of ERK inhibitor associated dermatologic adverse events: analysis from a nonrandomized trial of ulixertinib for advanced cancers. *Invest New Drugs***39**, 785-795 (2021). <https://doi.org:10.1007/s10637-020-01035-9>
23. Hakim, S., Craig, J. M., Koblinski, J. E. & Clevenger, C. V. Inhibition of the Activity of Cyclophilin A Impedes Prolactin Receptor-Mediated Signaling, Mammary Tumorigenesis, and Metastases. *iScience***23**, 101581 (2020). <https://doi.org:10.1016/j.isci.2020.101581>
24. Li, Y. & Yang, L. Cyclophilin a represses reactive oxygen species generation and death of hypoxic non-small-cell lung cancer cells by degrading thioredoxin-interacting protein. *Cell Cycle***21**, 1996-2007 (2022). <https://doi.org:10.1080/15384101.2022.2078615>

25. Wang, S., Li, M., Xing, L. & Yu, J. High expression level of peptidylprolyl isomerase A is correlated with poor prognosis of liver hepatocellular carcinoma. *Oncol Lett***18**, 4691-4702 (2019).
<https://doi.org/10.3892/ol.2019.10846>
26. Awad, M. M. *et al.* Acquired Resistance to KRAS(G12C) Inhibition in Cancer. *N Engl J Med***384**, 2382-2393 (2021). <https://doi.org/10.1056/NEJMoa2105281>
27. Zhao, Y. *et al.* Diverse alterations associated with resistance to KRAS(G12C) inhibition. *Nature***599**, 679-683 (2021). <https://doi.org/10.1038/s41586-021-04065-2>
28. Ho, C. S. L. *et al.* HER2 mediates clinical resistance to the KRAS(G12C) inhibitor sotorasib, which is overcome by co-targeting SHP2. *Eur J Cancer***159**, 16-23 (2021).
<https://doi.org/10.1016/j.ejca.2021.10.003>
29. Ryan, M. B. *et al.* Vertical Pathway Inhibition Overcomes Adaptive Feedback Resistance to KRAS(G12C) Inhibition. *Clin Cancer Res***26**, 1633-1643 (2020). <https://doi.org/10.1158/1078-0432.CCR-19-3523>
30. Kwan, A. K., Piazza, G. A., Keeton, A. B. & Leite, C. A. The path to the clinic: a comprehensive review on direct KRAS(G12C) inhibitors. *J Exp Clin Cancer Res***41**, 27 (2022).
<https://doi.org/10.1186/s13046-021-02225-w>
31. Ostrem, J. M. & Shokat, K. M. Direct small-molecule inhibitors of KRAS: from structural insights to mechanism-based design. *Nat Rev Drug Discov***15**, 771-785 (2016).
<https://doi.org/10.1038/nrd.2016.139>
32. Ostrem, J. M., Peters, U., Sos, M. L., Wells, J. A. & Shokat, K. M. K-Ras(G12C) inhibitors allosterically control GTP affinity and effector interactions. *Nature***503**, 548-551 (2013).
<https://doi.org/10.1038/nature12796>
33. Nokin, M. *et al.* Novel RAS(ON) inhibitors overcome clinical resistance to KRAS G12C covalent blockade. *Manuscript Submitted*

Figures

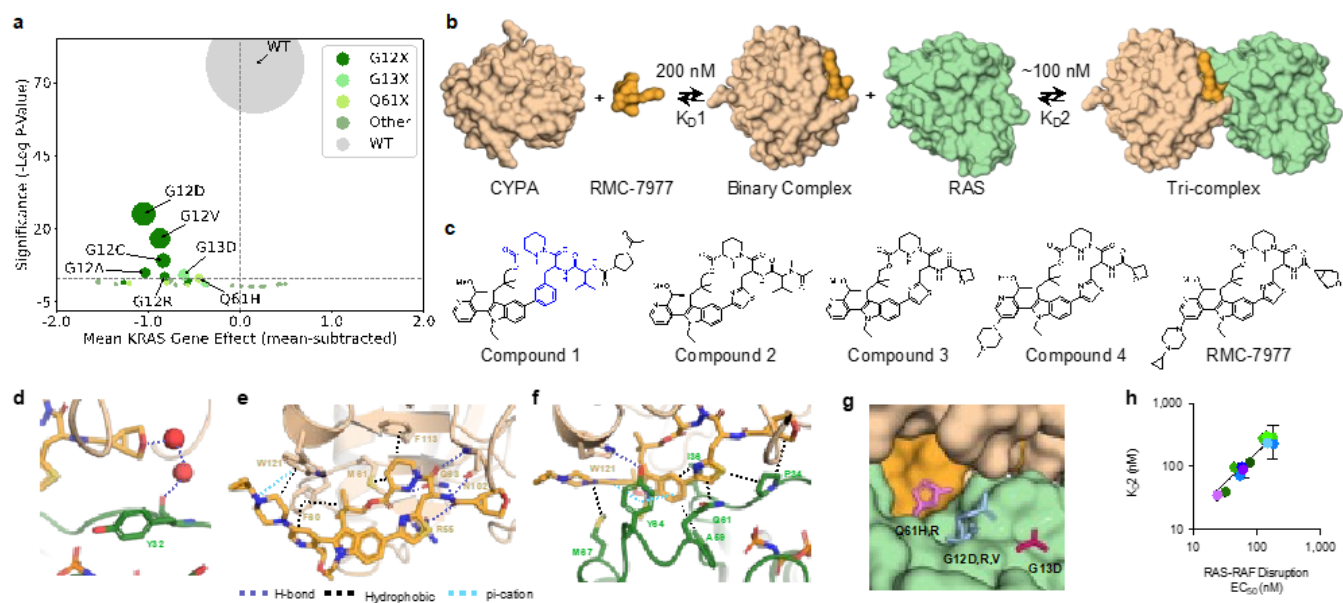


Figure 1

RMC-7977 inhibits the active state of multiple RAS variants.

a, Mean KRAS Chronos Effect score for each *KRAS* genotype is shown, with the mean effect score across all cell lines subtracted. P-values were calculated by a two-sided Wilcoxon rank sums test comparing the distribution of genotype effect to the distribution of effect scores outside of that genotype (Bonferonni-corrected p-value of $0.05 / 31 = 0.0016$ indicated by a gray horizontal line, 31 *KRAS* genotypes tested, point size is proportional to sample size of each genotype). **b**, Schematic of tri-complex formation showing reversible binding of RMC-7977 to CYPA (K_D1), and the binary complex to RAS (K_D2). **c**, Compound structures. Compound 1 CYPA-binding motif is highlighted in blue. **d**, Through-water hydrogen bonding network is formed between the ether of RMC-7977 and the carbonyl of RAS Y32. **e**, CYPA:RMC-7977 binding showing hydrogen bonds, including residue R55, the piperazic acid moiety, and residues F113 and M61, the geminal dimethyl group and F60, and the pyridine and F60. The basic nitrogen of the piperazine forms a cation-pi with W121 **f**, Oriented by the hydrogen bond to CYPA W121, RAS Y64 forms pi stacking interactions with the pyridine and indole groups. Apolar sidechains on both SWI and SWII form hydrophobic interactions with RMC-7977. **g**, The binding mode creates a groove along the Q61-G12-G13 axis. **h**, Correlation between K_D2 (SPR), and EC_{50} for disruption of RAS-RAF binding *in vitro* for wild-type and oncogenic RAS mutant proteins. Error bars indicate s.d. (*KRAS* variants in green, *NRAS* in blue, *HRAS* in purple; $m = 1.6 \pm 0.47$, $R^2 = 0.86$; values also shown in Extended Data Table 1).

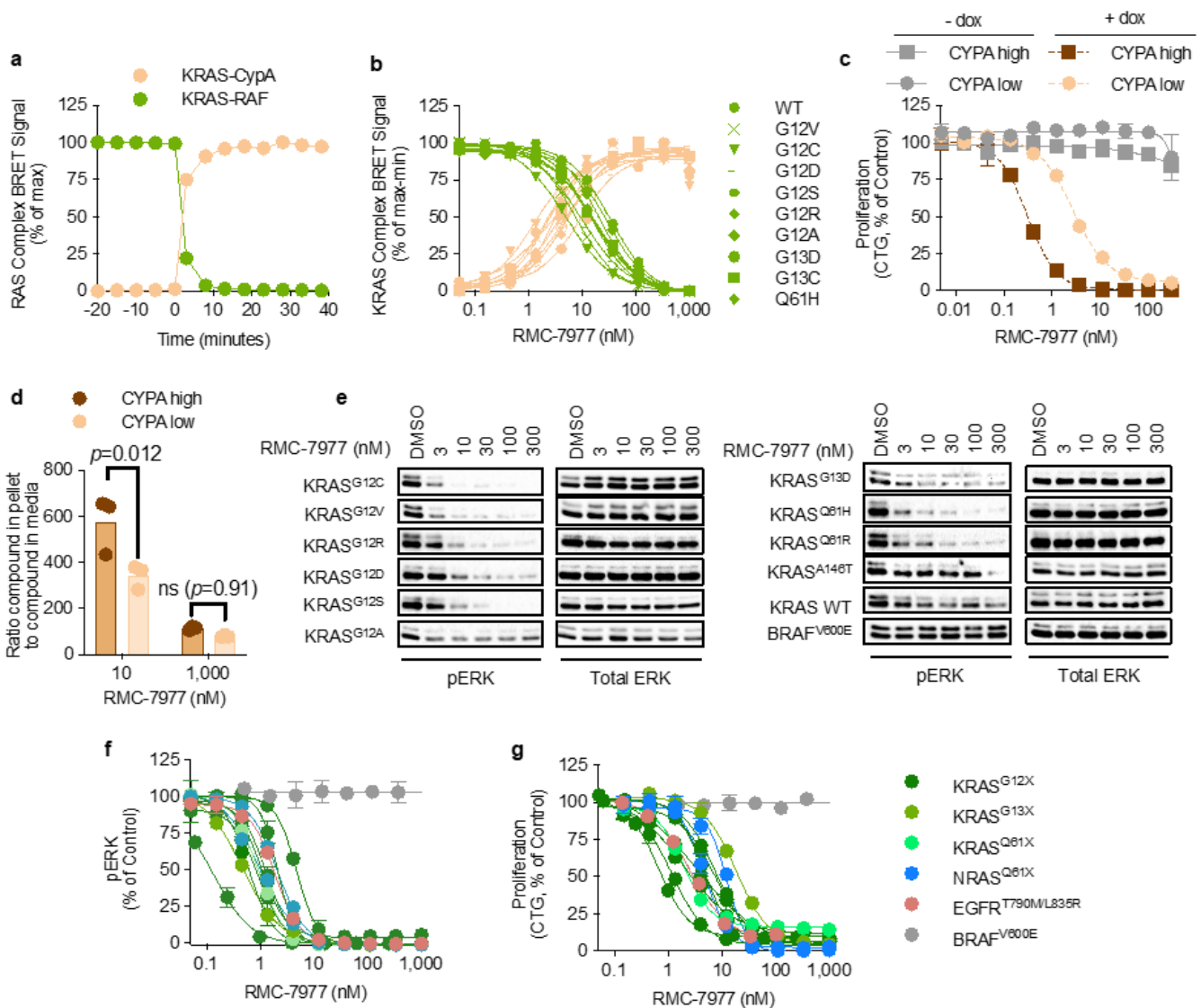


Figure 2

RAS inhibition is CYPA dependent and active against multiple RAS variants.

a,b Live-cell nano-BRET assay showing formation of the KRAS:CypA complexes (brown) and disruption of the KRAS:CRAF interaction (green) as a function of time after 50 nM RMC-7977 treatment (**a**), or RMC-7977 concentration (**b**). **c**, Cell proliferation (CTG) of NCI-H358 cells harboring doxycycline-inducible expression of low or high CYPA levels treated with RMC-7977 ± doxycycline (0.1 µg/ml) for 120 hours. Representative data shown of 2-3 independent experiments. Data points are the mean of technical duplicates normalized to vehicle control. Error bars indicate s.d. **d**, LC/MS measurements, ratio of RMC-7977 concentration in CYPA high and CYPA low NCI-H358 cells to concentration in media, 1 hour compound treatment (p values determined by one-way ANOVA with post hoc Tukey's test). **e**, Western blots of isogenic "RAS-less" MEF cells harboring wild-type (WT) or mutant *KRAS* or *BRAF*^{V600E}, treated with indicated concentrations of RMC-7977 or DMSO for 24 hours. pERK inhibition shown in all *KRAS* expressing cells. Total ERK used as a loading control. **f,g** pERK (AlphaLISA) (**f**) and proliferation (CTG) (**g**)

levels of human cancer cell lines with G12-mutant *KRAS* (Capan-1, SW620, AsPC-1, HPAC, NCI-H358, PSN-1, HUP-T3), G13 (HCT 116), and Q61 (Hs 766T); Q61-mutant *NRAS* (SK-MEL-30, KU1919); mutant *EGFR* (NCI-H1975) or *BRAF*^{V600E} (A375), treated with indicated concentrations of RMC-7977 for 4 hours. Representative data shown of 2-26 independent experiments. Data points represent the mean of technical duplicates normalized to vehicle control. Error bars indicate s.d.

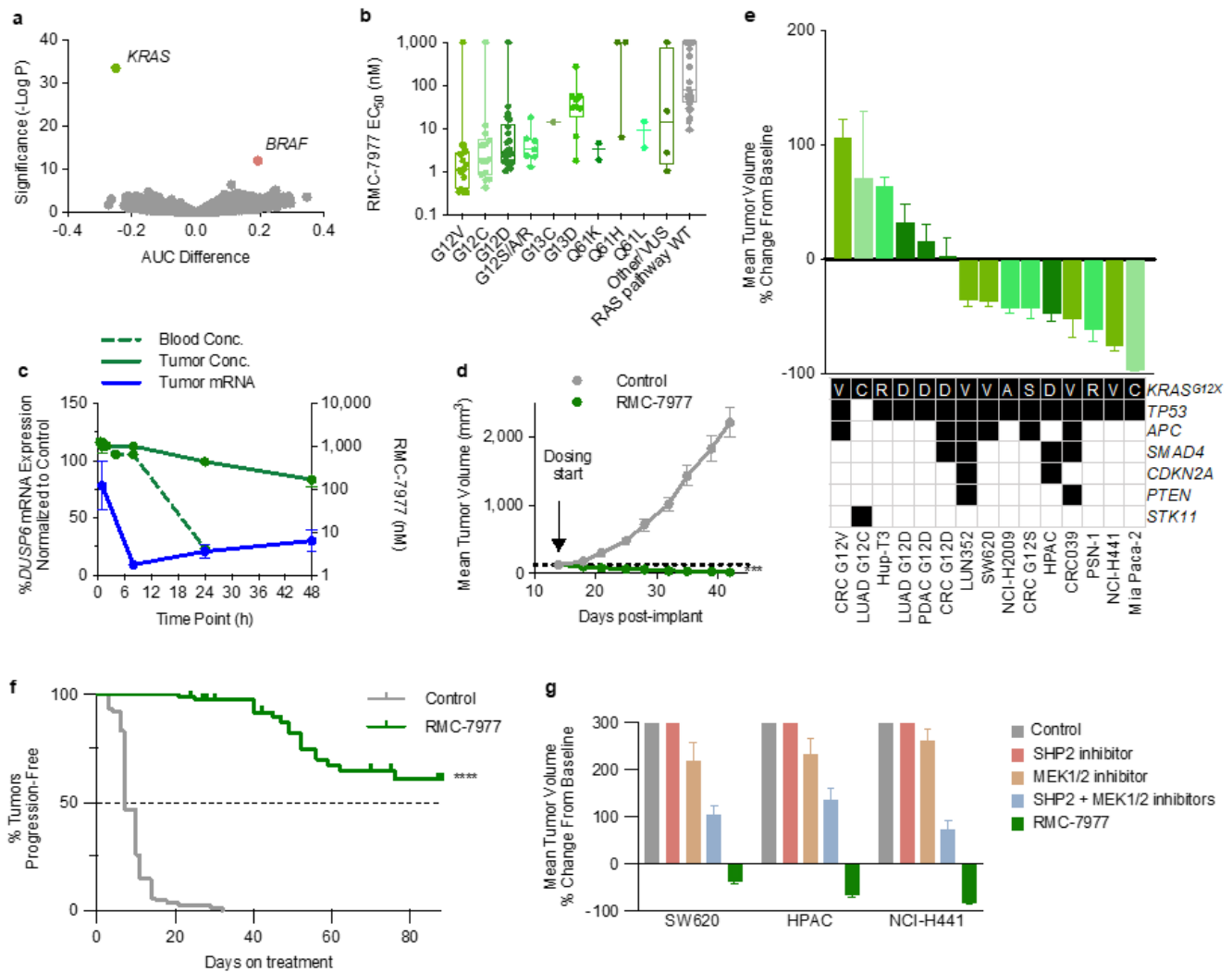


Figure 3

RMC-7977 is broadly active in RAS-addicted cancer models.

a, PRISM assay data showing RMC-7977 area under the curve (AUC) difference (x-axis) and significance (y-axis) between cell lines with and without a given gene mutation. Points represent mutated genes. A negative AUC indicates increased sensitivity to RMC-7977 and positive AUC indicates resistance. **b**, PRISM data showing RMC-7977 EC₅₀ as a function of *KRAS* genotype. Each point represents a cell line. Median EC₅₀: *KRAS*^{G12V} (1.15 nM), *KRAS*^{G12C} (1.84 nM), *KRAS*^{G12D} (2.86 nM), *KRAS*^{G12S/A/R} (3.24 nM),

KRAS^{G13D} (31.6 nM), *KRAS*^{G13C} (14.1 nM), *KRAS*^{Q61K,H,L} (3.22 nM, >1 μM, 9.00 nM, respectively), and *KRAS*^{Other/VUS} (13.9 nM). **c**, Blood (dotted line) and tumor (solid line) concentrations of RMC-7977 (green) and *DUSP6* mRNA level (blue) in NCI-H441 xenograft tumors following a single 10 mg/kg dose of RMC-7977. Error bars indicate s.e.m. **d**, Mice bearing NCI-H441 CDX tumors were treated with RMC-7977 at 10 mg/kg po qd for 28 days. ***adj. p<0.001 2-way ANOVA (n=8/group) adjusted via Dunnett's test on the final tumor measurement. Dotted line indicates initial average tumor volume. Error bars indicate s.e.m. **e**, Xenograft tumor models were treated with RMC-7977 (10 mg/kg po qd) for 4-6 weeks. Error bars indicate s.e.m. Table shows select genotypes with the top row indicating the *KRAS* genotype. **f**, Kaplan-Meier analysis of *KRAS*^{G12X} mutant CDX and PDX models treated with RMC-7977 10 mg/kg qd po. Time to event determined by the time on treatment to tumor size doubling. **g**, CDX models treated with the vehicle Control, SHP2 (RMC-4550 20 mg/kg po q2d), MEK (cobimetinib 2.5 mg/kg po qd), combination of SHP2 + MEK inhibitors (RMC-4550 20 mg/kg po q2d + cobimetinib 2.5 mg/kg po qd), or RMC-7977 at 10 mg/kg po qd. NCI-H441 (*KRAS*^{G12V} NSCLC) and HPAC (*KRAS*^{G12D} PDAC) models were treated for 21 days. SW620 (*KRAS*^{G12V} CRC) was treated for 28 days. Error bars indicate s.e.m.

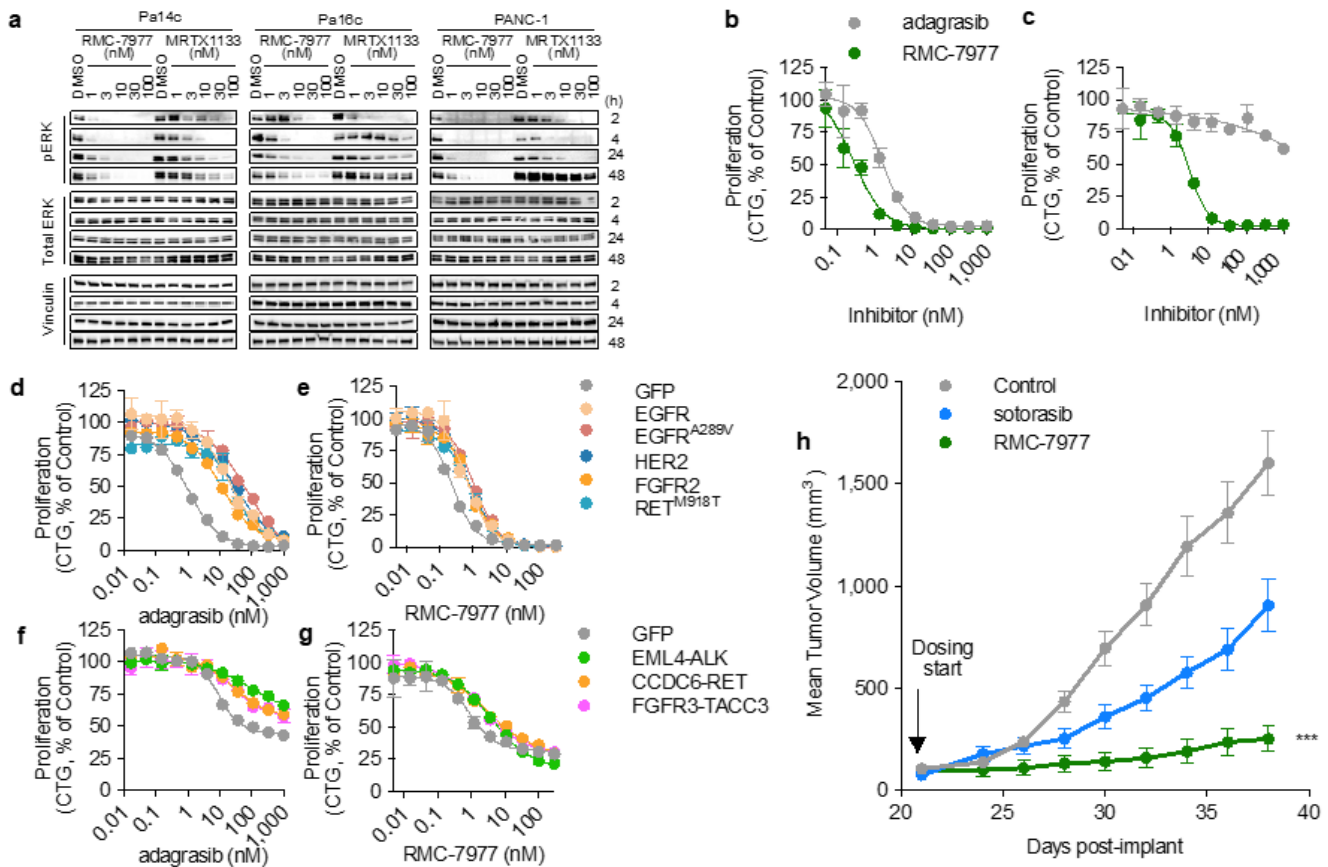


Figure 4

RMC-7977 can overcome resistance to mutant selective KRAS inhibition.

a, RAS signaling western blot time course of *KRAS*^{G12D} mutated PDAC cell lines treated with the indicated

concentrations of RMC-7977, MRTX1133, or DMSO control. pERK inhibition for both compounds shown at 2, 4, 24, and 48 hours. Total ERK and vinculin used as a loading controls. **b,c** Parental NCI-H358 cells (*KRAS*^{G12C}, NSCLC) (**b**) and adagrasib resistant NCI-H358 cells with a secondary *NRAS*^{Q61K} mutation (**c**) were treated with the indicated concentrations of adagrasib or RMC-7977 for 5 days and proliferation was measured by CTG. Error bars indicate s.d. **d,e** NCI-H358 (*KRAS*^{G12C}, NSCLC) cells expressing exogenous RTK DNA constructs indicated by color (GFP control, wild-type EGFR, EGFR^{A289V}, HER2, FGFR2, or RET^{M918T}, treated with adagrasib (**d**) or RMC-7977 (**e**) for 120 hours. **f,g** MIA PaCa-2 (*KRAS*^{G12C}, PDAC) cells expressing exogenous RTK fusion DNA constructs indicated by color (GFP control, EML4-ALK, CDC6-RET, FGFR3-TACC3), treated with adagrasib (**f**), or RMC-7977 (**g**) for 120 hours. Error bars indicate s.d. **h**, Patient-derived xenograft model established from a *KRAS*^{G12C} NSCLC patient who developed resistance after sotorasib. Mice were treated with vehicle, sotorasib (50 mg/kg po qd), or RMC-7977 (10 mg/kg po qd). Tumor volumes were assessed for 17 days after treatment started. ***adj. $p < 0.001$ for RMC-7977 vs control group, using repeated measures 2-way ANOVA (n=7-10/group) adjusted based on multiple comparison via Dunnett's test on the final tumor measurement. Error bars indicate s.e.m.

Supplementary Files

This is a list of supplementary files associated with this preprint. Click to download.

- [SupplementaryTable17977crysyallography.xlsx](#)
- [SupplementaryTable2PRISMpanel.xlsx](#)
- [SupplementaryTable3183celllinepanelEC50.xlsx](#)
- [RMC7977Methods.docx](#)
- [ExtendedDataFigs.docx](#)